Optics & Laser Technology 44 (2012) 948–953

Contents lists available at SciVerse ScienceDirect

Optics & Laser Technology

journal homepage: www.elsevier.com/locate/optlastec

Damage/ablation morphology of laser conditioned sapphire under 1064 nm laser irradiation

Y. Jiang [a,b], X. Xiang [a,*], H.J. Wang [b], X.D. Yuan [b], S.B. He [b], H.B. Lv [b], W.G. Zheng [b], X.T. Zu [a,**]

[a] Department of Applied Physics, University of Electronic Science and Technology of China, Chengdu 610054, PR China
[b] Research Center of Laser Fusion, China Academy of Engineering Physics, Mianyang 621900, PR China

ARTICLE INFO

Article history:
Received 22 April 2011
Received in revised form
23 October 2011
Accepted 1 November 2011
Available online 21 November 2011

Keywords:
Sapphire
Laser conditioning
Damage/ablation morphology

ABSTRACT

The damage/ablation morphologies and laser induced damage threshold (LIDT) of three different sapphire samples: original, 1064 nm laser conditioned and 10.6 μm CO_2 laser polished substrates are investigated with ns pulses laser irradiation. The results indicate that the damage resistance capability cannot be enhanced by 1064 nm laser conditioning or CO_2 laser polishing. The damage/ablation morphology of 1064 nm-laser conditioned samples is same as that of the original sapphire. But it is different from the damage/ablation morphology of the CO_2 laser polished sapphire. The "gentle and strong" ablation phases are observed in this work and several phenomena are observed in the two ablation phases. Ripple is observed in the "gentle" ablation processes, while convex spots and raised rims are observed in the "strong" ablation processes. Meanwhile, stripe damage and pin-points are observed in the CO_2 laser conditioned sapphire after ns laser irradiation. The formation mechanisms of the phenomena are also discussed for the explanation of related damage/ablation morphology. The results may be helpful for the damage/ablation investigation of sapphire in high power laser systems.

1. Introduction

The surface ablation (material removal) and surface damage threshold or morphology of optical materials, e.g., sapphire, fused silica and potassium dihydrogen phosphate (KDP) crystal, have been extensively studied under laser irradiation with various pulse widths and wavelengths [1–6]. Sapphire is a popular and suitable material in many fields because of the wide band-gap of ~8.8 eV [7,8]. It is a well investigated material due to its many useful mechanical, optical and electrical properties for the development of high power laser technology at various wavelengths [9]. It has been widely used as both windows and substrates in demanding environments, such as dynamic shock wave experiments induced by intense laser illumination [4,10], to transmit probe or drive lasers and to produce and sustain high loading stress [4].

Extensive studies have been conducted to investigate structural modification, damage/ablation morphology and mechanisms of sapphire under ultra-short pulse (fs [9,11,12], ps [2,13,14]) laser irradiation. However, there are few reports on long pulse laser irradiation. The reports mainly focus on the LIDT of sapphire under ns [7,12,15] or μs [4] pulse regime. It is reported that the LIDT of sapphire depends on the pulse duration [16]. A weak dependence of the LIDT fluence versus wavelength in the explored range 532–1064 nm was reported by Uteza et al. and they ascribed the weak relationship to the large band gap of sapphire (8.8 eV) with respect to the photon energy range (1.2–2.3 eV) [12]. They also reported the differences of laser–matter interaction and laser-damage mechanisms between the short pulse (fs and ps) and long pulse (ns). The results suggested that the short pulse experiments showed a good reproducibility at a given fluence, which makes the determination of the diameter of the damage effected zone easy and unambiguous. On the contrary, the long pulse experiments do not allow such a precise determination, the damage occurrence being not systematic at a given fluence [7,12].

In this work, we focus on the morphology of ablation craters and damage created in the different laser conditioned sapphire samples with a fixed pulse duration of 11.7 ns and fixed wavelength of 1064 nm single mode Nd:YAG laser. The sapphire samples are original, 1064 nm Nd:YAG conditioned and 10.6 μm CO_2 laser polished ones. Two ablation phases are observed in the different conditioned samples. Different phenomena such as ripple, raised rim, convex spots are observed at "gentle" or "strong" ablation processes, and stripe damage and pin-points are observed in the CO_2 laser polished samples. The results provide a reference to identify the damage morphology of sapphire used in high power laser systems and to understand the damage mechanisms.

* Corresponding author. Tel./fax: +86 28 83202130.
** Corresponding author. Tel./fax: +86 28 83201939.
E-mail addresses: xiaxiang@uestc.edu.cn (X. Xiang), xtzu@uestc.edu.cn (X.T. Zu).

0030-3992/$ - see front matter © 2011 Elsevier Ltd. All rights reserved.
doi:10.1016/j.optlastec.2011.11.003

2. Experimental details

Sapphire samples with size of 20 mm in diameter are used in this work, and the samples are divided into three groups, labeled Groups A, B and C. Group A samples are original sapphire without any treatment. Groups B and C are conditioned by raster scanning with a 1064 nm, 11.7 ns single mode Nd:YAG laser and a 10.6 μm CO_2 laser. The scanning pattern of laser conditioning is shown in Fig. 1. The laser beams overlap ratio is 50% and the fluence or power increases gradually during the scanning process. For the 1064 nm laser scanning process, the maximum fluence is less than the damage/ablation threshold of sapphire. For the CO_2 laser scanning process, the start scan power is 30 W, and the increment of power is 2 W after each scan loop, up to 50 W. It can effectively avoid fracture induced by temperature difference between laser affected and un-affected areas during scanning. Moreover, residual surface contaminations and polishing defects can be removed during the laser polishing processes [17].

The damage/ablation threshold is tested with R/1 procedure (irradiating the same area with a number of pulses at a repetition rate [18,19]) at the same laser parameters (wavelength, beam radius) for three groups before and after laser conditioning. The damage/ablation tests were conducted using the 1064 nm signal mode Nd:YAG laser with pulse width of 11.7 ns. The schematic diagram of the experimental setup for damage/ablation test is shown in Fig. 2. The laser beam is a spatial near-Gaussian distribution with beam area of 1 mm^2 at $1/e^2$. The incident angle of laser is less than 5°. The beam areas are characterized by a science CCD camera and a Spiricon beam analyzer successively in far-field using a long focal length lens.

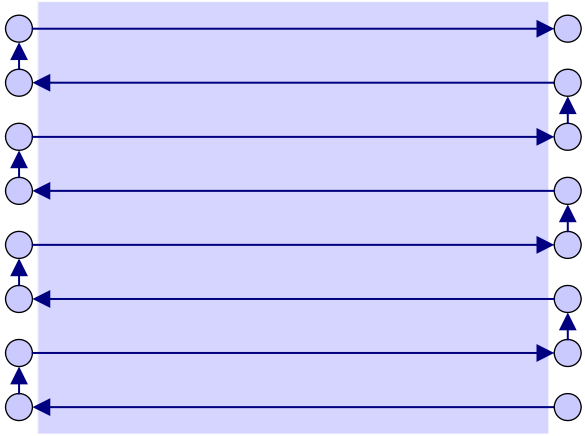

Fig. 1. Schematic scanning pattern of 1064 nm Nd:YAG and 10.6 μm CO_2 laser conditioning.

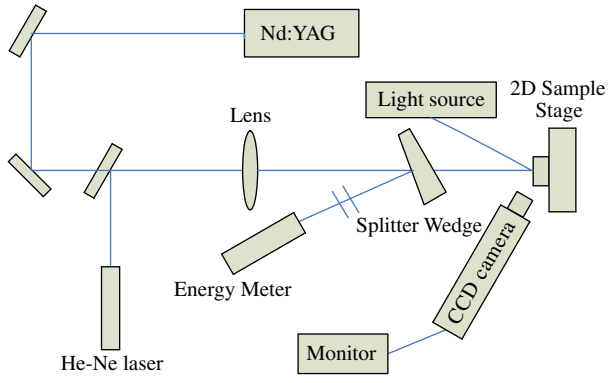

Fig. 2. Schematic diagram of experimental setup for LIDT test.

The measurement is repeated several times to obtain the average beam dimensions. The laser fluence fluctuates less than 5%. An EMP 1000 energy meter is used to collect the energy data of each shot. A science CCD camera is used to monitor the initial damage/ablation in several microns in the surface of sapphire samples. The 30° viewing angle allows the in-situ observation of rear-surface modifications to the sample. In addition, a cw-He:Ne laser is used to monitor the optical alignment, also illuminate the processed target area on the sample. In this work, we define that the damage threshold as the ablation threshold. In other words, the irradiated zone is damaged if the ablation is observed by the CCD camera, and the fluence is regarded as damage/ablation threshold.

Three methods are employed to analyze the front and rear surface morphology after laser irradiation. A Nikon E600 optical microscopy is utilized to observe the surface defects of samples before test and characterize the affected zone (dimensions, morphology) after test. A Zygo FPM-1000 profilometer and an atom force microscopy (AFM) provide the detailed profile information of the damage/ablation craters.

3. Results and discussion

Uteza et al. reported the LIDT in the ns regime of sapphire cannot be precisely determined but show a statistical nature because of the linear absorption of randomly scattered impurities and defects [7]. In this study, the statistical average LIDTs for Groups A, B and C are 22.5 J/cm^2, 26.5 J/cm^2 and 21.8 J/cm^2, respectively. The results indicate that there is no clear improvement of damage resistance capability by laser conditioning. It is different from the results on fused silica and KDP. IR or UV laser conditioning can effectively increase the LIDT of fused silica [20,21] and KDP [22]. The possible reasons may be related to the high hardness and high melting point (2323 K [8]) of sapphire. However, the damage/ablation morphology is different after different laser conditioning. The damage/ablation morphology of Group A (without any treatment) is same as that of Group B (1064 nm Nd:YAG laser conditioned). However, the damage/ablation morphology of Group C (10.6 μm CO_2 laser conditioned) is different from those of Groups A and B. Thus two kinds of damage/ablation morphologies are presented in Sections 3.1 and 3.2.

3.1. Ablation morphology of Groups A and B

The ablation morphologies of Groups A and B are shown in Fig. 3. Two ablation phases are observed from the images: "gentle" ablation (Fig. 3a) and "strong" ablation (Fig. 3b and c), consistent with the previous studies [1,9]. There are two major unsmooth (Fig. 3a and b) and smooth (Fig. 3c) craters. Furthermore, the unsmooth craters can also be divided into the irregular (Fig. 3a) and regular (Fig. 3b) craters. The typical surface morphology and profile of ablation craters measured by the profilometer are shown in Fig. 4. For all the ablation craters, the profile shows a spatial near-Gaussian distribution. It should be related to the spatial near-Gaussian distribution of the laser beam. There is a clear raised rim around the ablation crater in Fig. 4, and the raised rim is observed mainly in the "strong" ablation craters.

Some periodic ripples can be observed in the ablation area in Fig. 3(a), which also appears in the regular ablation craters. There are two kinds of ripples: annular and straight lines shown in Fig. 5 measured by AFM. The ripples can be easily observed at the central area compared with the edge of the crater, and the spacing of straight ripples is more uniform than that of the annular ripples. The average depth and spacing straight ripple is 20 nm and 8.5 μm, respectively. It is reported that the periodic structure